

Evidence of recurrent mass movement in front of the maximum slip area of the 1960 Chile earthquake: Implications for risk assessment and paleoseismology

Cristian Araya-Cornejo¹, Matías carvajal², Jasper Moernaut³, Felipe González⁴, and Marco Cisternas⁵

¹Pontifical Catholic University of Chile

²Universidad de Concepción

³University of Innsbruck

⁴RWTH AACHEN UNIVERSITY

⁵Pontificia Universidad Católica de Valparaíso

November 25, 2022

Abstract

We present evidence that suggests a new risk scenario for the Valdivia basin in south Chile, located in the area of the magnitude 9.5 1960 earthquake. In 1960, three mass movements, triggered by the earthquake shaking, dammed the upper course of the San Pedro River and threatened Valdivia City until it was opened in a controlled manner by its inhabitants. Published historical accounts indicate that the 1575 earthquake, predecessor of the 1960 event, also triggered a mass movement that dammed the upper course of the river. However, here we reinterpret the published account and present new historical records, which we combined with satellite imagery and field surveys to show that the volume of the landslide in 1575 was smaller than the smallest of those of 1960, yet its outburst flood killed thousands of natives located downstream. Additionally, we characterized different mass movement deposits in the upper course of the San Pedro River, including both ancient and those formed in 1960, and we evaluated the mechanisms that could contribute to their generation at present (e.g. land use). Our results suggest that in the present-day conditions a moderately-sized ($M_w \sim 8$) earthquake can be sufficient to cause damming the San Pedro River, which challenges the previous assumption that such phenomena are exclusively related to giant 1960-like earthquakes.

Hosted file

supporting information araya et al. for jgr.docx available at <https://authorea.com/users/553844/articles/605370-evidence-of-recurrent-mass-movement-in-front-of-the-maximum-slip-area-of-the-1960-chile-earthquake-implications-for-risk-assessment-and-paleoseismology>

1 **Evidence of recurrent mass movement in front of the maximum slip area of the 1960**
2 **Chile earthquake: Implications for risk assessment and paleoseismology**

3 **Cristian Araya-Cornejo^{1,2}, Matías Carvajal³, Jasper Moernaut⁴, Felipe González⁵, Marco**
4 **Cisternas^{3,6}**

5 ¹Instituto de Geografía, Pontificia Universidad Católica de Chile, Chile

6 ²Observatorio de Gestión de Riesgo de Desastres, Universidad Bernardo O'Higgins, Chile

7 ³Millennium Nucleus The Seismic Cycle Along Subduction Zones, Chile

8 ⁴Institute of Geology, University of Innsbruck, 6020 Innsbruck, Austria

9 ⁵Chair for Computational Analysis of Technical Systems, RWTH Aachen University, Germany

10 ⁶Instituto de Geografía, Pontificia Universidad Católica de Valparaíso, Chile

11

12 Corresponding author: Cristian Araya-Cornejo (c.arayacornejo@gmail.com)

13

14 **Key Points:**

- 15 • Historic and geomorphic evidence reveals several mass movements triggered by
16 earthquakes on a riverside zone in south Chile.
- 17 • Giant earthquakes in 1575 and 1960 triggered mass movements causing river damming,
18 but those of the latter were larger in quantity and size.
- 19 • Evidence presented here suggest rethinking near-future hazards and risks in the Valdivia
20 basin.

21 **Abstract**

22 We present evidence that suggests a new risk scenario for the Valdivia basin in south Chile,
23 located in the area of the magnitude 9.5 1960 earthquake. In 1960, three mass movements,
24 triggered by the earthquake shaking, dammed the upper course of the San Pedro River and
25 threatened Valdivia City until it was opened in a controlled manner by its inhabitants. Published
26 historical accounts indicate that the 1575 earthquake, predecessor of the 1960 event, also
27 triggered a mass movement that dammed the upper course of the river. However, here we
28 reinterpret the published account and present new historical records, which we combined with
29 satellite imagery and field surveys to show that the volume of the landslide in 1575 was smaller
30 than the smallest of those of 1960, yet its outburst flood killed thousands of natives located
31 downstream. Additionally, we characterized different mass movement deposits in the upper
32 course of the San Pedro River, including both ancient and those formed in 1960, and we
33 evaluated the mechanisms that could contribute to their generation at present (e.g. land use). Our
34 results suggest that in the present-day conditions a moderately-sized ($M_w \sim 8$) earthquake can be
35 sufficient to cause damming the San Pedro River, which challenges the previous assumption that
36 such phenomena are exclusively related to giant 1960-like earthquakes.

37 **1 Introduction**

38 Gravitational mass movements (including landslides) are a significant hazard in most countries
39 (Keefer and Larsen, 2007). Although the triggering of mass movements (MM) depends on
40 different factors (e.g. heavy rains), earthquakes are documented as their main trigger when
41 seismic shaking reaches a Modified Mercalli Intensity ($MMI \geq VI$) (Keefer, 1984). The recent
42 history of tectonically active zones shows that earthquake-triggered MM have caused tens of
43 thousands of deaths in densely populated areas (Budimir et al., 2014), and are one of the
44 consequences of earthquakes that have caused greatest economic losses (Alexander, 2012).
45 Additionally, earthquake-triggered MM have the potential for triggering cascading hazards (e.g.
46 damming rivers, tsunamis) amplifying its potential effect (Budimir et al., 2014). An example of
47 this are the recent tsunamis following the M_w 7.5 2018 Palu earthquake (Indonesia), which were
48 generated by a combination of submarine/subaerial MM and coseismic seafloor deformation,
49 killing thousands of people (Carvajal et al., 2019).

50 The preconditioning of slopes towards failure can be influenced by various secondary factors
51 independent of the ground shaking. These include terrain parameters like morphology (e.g. slope
52 angle and curvature), slope materials (e.g. soil cover, lithology and geological structure),
53 hydrology (e.g. water table level and pore water pressure), geomorphology (e.g. presence of
54 ancient MM deposit) and anthropogenic (e.g. land use) conditions (Gorum et al., 2011). Despite
55 their inherent complexity, the empirically-derived causal relationships between earthquake size
56 and mass movements and the preservation of their deposits in the landscape (Keefer, 2013), has
57 allowed to use mass movement deposits as proxies to estimate the ages and magnitude ranges of
58 historical and prehistoric earthquakes (Ojala et al., 2017). Thus, scientific work focused on
59 improving the inventory of earthquake-triggered MM deposits (e.g. spatio-temporal distribution),
60 and/or on characterizing their forcing mechanisms (e.g. terrain parameters), can provide critical
61 information for the assessment of seismic hazard in areas affected by these phenomena (Harp et
62 al. 2011).

63 Chile is located over one of the most active subduction zones in the world and has one of the
64 higher rates of earthquake occurrence, with an average of two $M_w \geq 8.4$ per century (Ruiz and
65 Madariaga, 2018). Although most of the great earthquakes ($M_w > 8$) are sourced in the
66 megathrust fault formed by the South American and Nazca plates, intraplate faults (e.g. within
67 either plate) have also generated large magnitude events ($M_w > 6$) with associated strong shaking
68 capable of producing MM (Antinao and Gosse, 2009). The M_w 6.2 2007 shallow crustal
69 earthquake in the southern part of the country and its cascading effects provide a remarkable
70 example. Rupturing a ~50 km-long segment of the Liquiñe-Ofqui strike-slip fault (Agurto et al.,
71 2012), this earthquake triggered multiple landslides (e.g. rock slides, rock avalanches, slumps,
72 slow earth flows, others) that entered the Aysén Fjord generating tsunamis that killed a dozen of
73 people (Sepúlveda et al., 2010), highlighting the urgent need of better understanding earthquake-
74 induced MM in Chile and their associated potential hazards. However, aside from a few other
75 MM studies focused on the $M_w \sim 9.5$ 1960 (Davis and Karzulovic, 1961; Weischet, 1963; Wright
76 and Mella, 1963) and M_w 8.8 2010 (Mardones and Rojas, 2012; Serey et al., 2019) earthquakes,
77 research on this topic in Chile is scarce. The upper course of the San Pedro River (39.7° S, 72.4°
78 W), which originates in the Riñihue Lake, faces the area of maximum slip of the giant (M_w 9.5)
79 1960 earthquake. This river and lake became the focus of attention after three remarkable MM
80 triggered by the strong 1960 earthquake shaking dammed it. As water accumulated upstream the
81 uppermost dam, the pressure induced to it increased, posing a time-increasing threat to the
82 population living downstream. Fortunately, when the Riñihue Lake level reached about ~26 m
83 above the typical water level, successful interventions led by the Chilean government with
84 the collaboration of the inhabitants of the basin (e.g. Valdivia and Los Lagos city inhabitants),
85 prevented an imminent collapse saving tens of thousands of people (Davis and Karzulovic,
86 1961). A similar story had occurred almost four centuries before, although with more tragic
87 consequences. The historic earthquake of 1575 identified as the predecessor of the 1960
88 earthquake (Cisternas et al., 2005), also triggered MM that dammed the San Pedro River.
89 However, aborigines living downstream by the time did not face the same destiny. After
90 “*months*” of water accumulation and over ~50 m of water level increase, the dam collapsed and
91 killed “*hundreds*” of them (Montessus de Ballore, 1912). Today, the MM deposits triggered by
92 both earthquakes are identifiable on the land surface and/or along the riverside, and their process
93 and geomorphology has not been investigated in detail. These deposits are the main focus of this
94 paper.

95 Here we improve the knowledge of earthquake-triggered MM in Chile by an in-depth study of
96 the MM deposits triggered by the 1960 and 1575 giant earthquakes in the upper course of the
97 San Pedro River. Through field observations and satellite imagery combined with newly found
98 historical accounts, we identify the deposits of both events and compare them with previous
99 reports. We further construct a high-resolution terrain model to study their characteristics at
100 different spatio-temporal scales. Finally, we review the potential factors controlling their
101 triggering and discuss the implications of modern land use on the geological hazards in the area.

102 2 Study Area

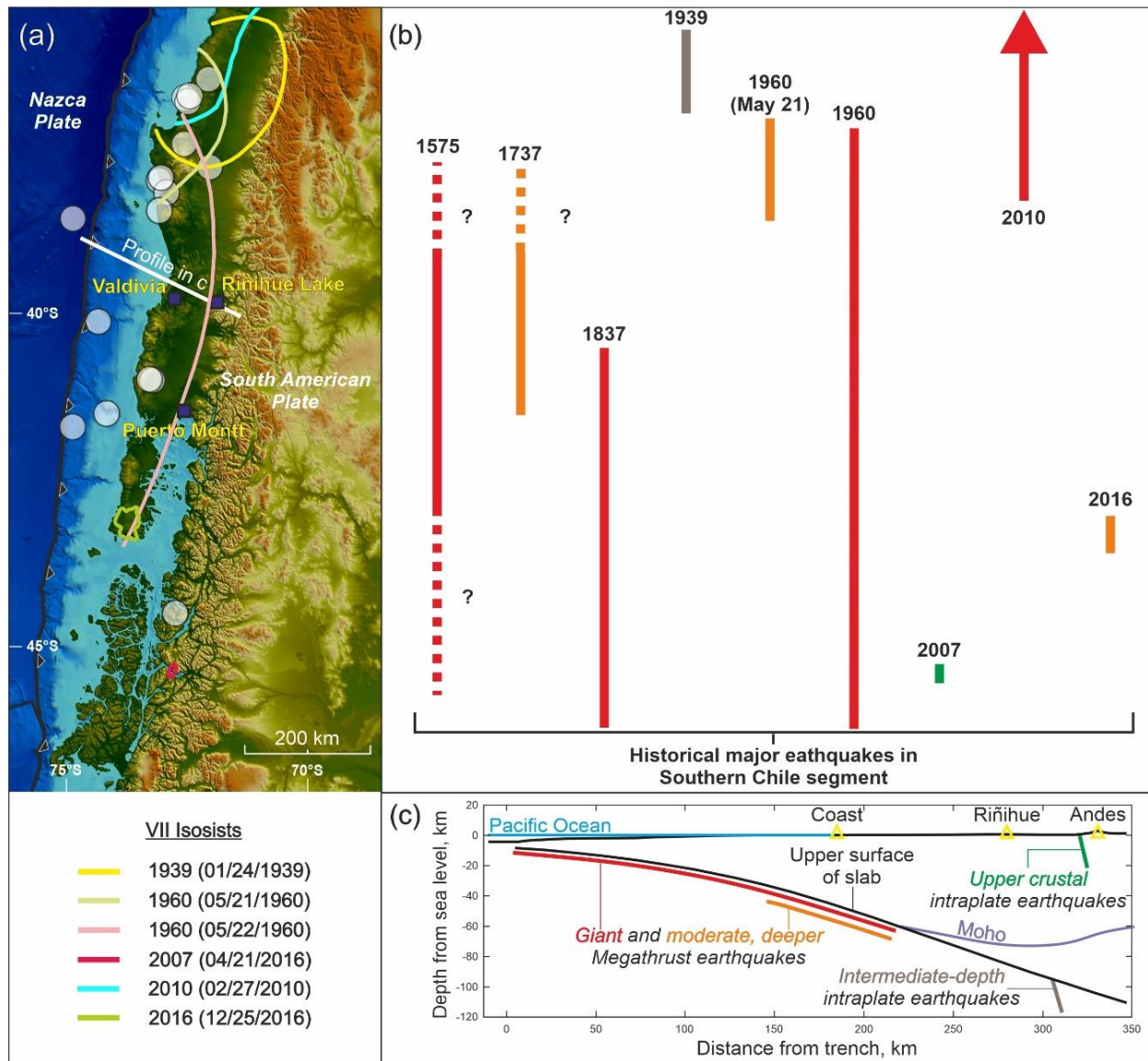
103 2.1 Geographical and seismotectonic setting

104 The San Pedro River and Riñihue Lake are located in the foothills of the Andes, about 280 km
105 south from the northern end of the 1960 rupture area (Figure 1). It originates in the outflow of

106 Riñihue Lake and flows into the Pacific Ocean (named Valdivia River). The upper course of the
107 river exhibits geographic and geological characteristics that pose potential hazards for the
108 population living downstream (~160.000 people). Its hydrographic catchment is composed of
109 seven other lakes, five in Chilean territory and two in Argentina, covering an area of ~450 km²
110 (Figure 2a). The interconnected system of lakes has a pluvio-nival regime and the river is
111 naturally regulated by these, which generates that a large part of the sediment load transported
112 from the upper catchment is deposited on the bottom of the lakes. For this reason, the San Pedro
113 River has crystal clear waters (Habit and Parra, 2012). Given the extensive hydraulic catchment
114 and their precipitation regime (~2200 mm/yr), landslide damming of San Pedro River could lead
115 to a rapid accumulation of a vast amount of water, potentially leading to catastrophic outburst
116 floods.

117 The seismotectonic setting is located in the south-central part of the active subduction zone of
118 Chile, which extends for ~3200 km from the northern limit of the country (18.4° S) to the Taitao
119 Peninsula (46.5° S). Along this zone, the Nazca oceanic plate subducts under the continental
120 plate of South America at a relative convergence of ~65-70 mm/year (Angermann et al., 1999).
121 The frictional interaction between both plates induces internal stress and consequent elastic
122 deformation in the upper plate, which slowly accumulates through decades or centuries until it is
123 suddenly released by large megathrust earthquake ruptures (Scholz, 2002).

124 In the ~500 years of Chile's history, the southern segment of this subduction zone has generated
125 at least five major megathrust earthquakes, including the Mw 9.5 1960 event, the largest
126 instrumentally-recorded worldwide (Kanamori and Cipar, 1974). Other significant earthquakes
127 occurred in 1575, 1737, 1837 (Lomnitz, 1970; Cisternas et al., 2005) and recently in 2016 (Mw
128 7.6) (Figure 1a,b). Despite the relative temporal regularity between one event and the other,
129 independent analysis of historical documents (Cisternas et al., 2017a) and sedimentary records at
130 the coast (Cisternas et al., 2017b) and within inland lakes (Moernaut et al., 2014), indicate that
131 the 1960 earthquake was only rivaled by the 1575 earthquake in terms of magnitude and rupture
132 extent. In contrast, the smaller 1737 (M ~7.5-8) and 1837 (M ~8.5-9) earthquakes were limited to
133 the northern and southern two thirds of the 1960 rupture area (1000 km long), respectively
134 (Figure 1b) (Cisternas et al., 2017a). The recent well-instrumented 2016 earthquake, with a Mw
135 7.6 (Moreno et al., 2018), seems to be the smallest event of this historical sequence, rupturing a
136 small, deep patch on the megathrust between latitudes 43-43.5° S (Moreno et al., 2018). Besides
137 these large events, the seismic catalogue shows 26 poorly-constrained events since 1570 with
138 magnitudes apparently over M 7 (white circles in Figure 1a,b), which yield an average of 6.5
139 events per century in this area.



140 **Figure 1.** (a) Location of earthquakes larger than Magnitude 7 that struck South-Central Chile
 141 in the historical period 1570-2016 (National Seismological Center of Chile, 2019); and Isoleist
 142 VII of the intraplate earthquakes of 1939 (Astroza et al., 2002) and 2007 (Vanneste et al., 2018);
 143 and interplate earthquakes of 1960 (21 and 22 of May) (Astroza and Lazo, 2010), 2010 (Astroza
 144 et al., 2012), and 2016 (USGS, 2016). (b) Rupture lengths of the most significant well-
 145 investigated earthquakes along the region. The line colors represent the source type of the
 146 earthquakes shown in (c). Orange are moderate-size, deeper interplate earthquakes (1737
 147 (Cisternas et al., 2017a), May 21 1960 (Ruiz and Madariaga, 2018) and 2016 (Moreno et al.,
 148 2018)). Red are great earthquakes rupturing the entire seismogenic width (1575, 1960 (Cisternas
 149 et al., 2005) and 2010 (Moreno et al., 2012)). Green indicates the strike-slip rupture of the 2007
 150 earthquake along the Liquiñe Ofqui Fault Zone (Agurto et al., 2012). Light brown indicates the
 151 1939 intermediate-depth earthquake rupture within the subducted slab (Beck et al., 1998).

152 Although no strong shaking has been instrumentally recorded in the direct vicinity of the San
 153 Pedro River, its relatively close location to the different earthquake source types in Chile makes

154 it an exposed site for seismic shaking. Because it is located ~280 km from the trench and over
155 the local downdip limit of the megathrust seismogenic zone, it is exposed to great-to-giant
156 megathrust earthquakes ($M_w > 8.5$), rupturing the entire seismogenic zone width (e.g. 1960 and
157 2010 type earthquakes), but also to smaller ones ($M_w \sim 8$) if are generated by deep interplate
158 ruptures (e.g. $M_w 7.6$ 2016 earthquake). Although smaller in magnitude, earthquakes rupturing
159 near the bottom of the seismogenic zone are capable of producing strong, high frequency shaking
160 radiated from these interplate depths (Lay et al., 2012). The $M_w 7.6$ 2016 Melinka earthquake,
161 for example, caused MMI VII over its rupture area (USGS, 2019). According to Moreno et al.
162 (2018), earthquakes with these characteristics will continue to occur along this region while
163 strain energy builds-up for the next 1960-type earthquake. Additionally, because the San Pedro
164 River is only a few tens of kilometers from the trace of the Liquiñe-Ofqui strike-slip fault
165 zone, it can also be exposed to strong shaking from these events. The $M_w 6.2$ 2007 Aysén
166 earthquake, with the associated landslides and tsunami effects, represents a recent example of
167 this type of earthquakes. Strike-slip faults are well-known to cause very strong shaking ($> VIII$
168 MMI) near and around the rupture area, even in moderate-size earthquakes (Carver et al., 2004;
169 Colombelli et al., 2013; Symithe and Calais, 2016; Barnhart et al., 2019).

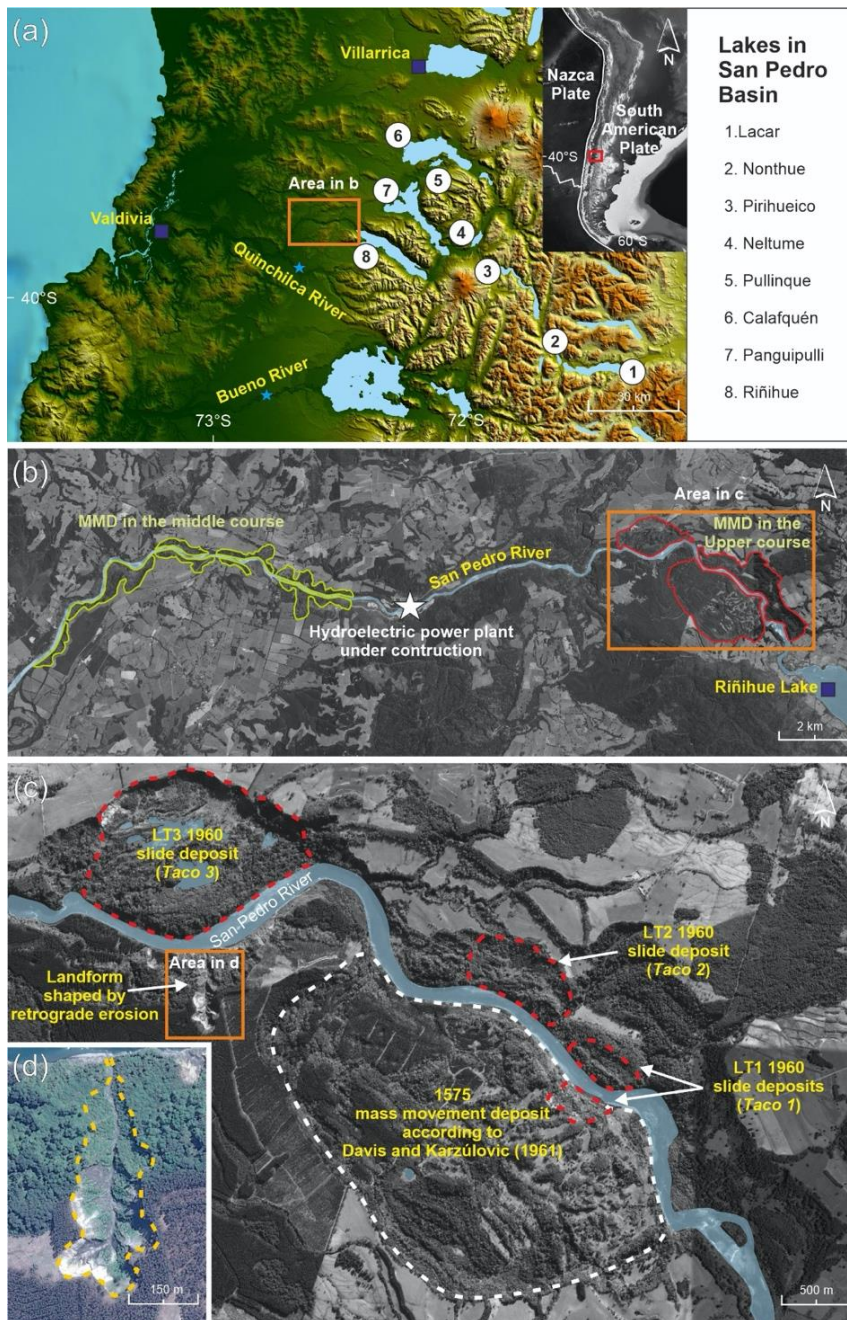
170 Finally, the San Pedro River is also exposed to potential shallow earthquakes originating at the
171 Andes foothill (e.g. Alvarado et al., 2009) and to intermediate depth events generated within the
172 downgoing slab (Beck et al., 1998) (Figure 1c). The latter type of events are capable to produce
173 very strong shaking with epicentral seismic intensity of up to MMI IX (Moya, 2002). In fact, the
174 largest seismic catastrophe in Chile, with about ~20.000 deaths, was caused by the $M_s \sim 7.8$
175 Chillán intermediate-depth earthquake (Beck et al., 1998; Ruiz and Madariaga, 2018).

176 2.2 Geological setting and previous work

177 The local geological setting of the upper course of the San Pedro River is a relevant factor to
178 explain the presence of MM deposits triggered by earthquakes. The riverside zones of its middle
179 and upper courses show multiple MM deposits, which cover an approximate area of 10 km^2
180 (Figure 2b). They are identifiable with any remote sensing tool due to their size and exhibit a
181 well demarcated outline. Some of these deposits are coalescent and show different degrees of
182 evolution, evidenced by their level of surface roughness and the escarpments slope gradients.
183 Also, these deposits can determine the sinuosity of the river. Due to their morphological features,
184 such as roughness and size, the MM deposits of the middle course of the San Pedro River are
185 clearly older and smaller than those present in the upper course (Figure 2b). Interestingly, these
186 phenomena have not been recorded either geomorphologically or historically in neighboring
187 basins of tributary rivers, despite their similar seismic exposure and climatic conditions (e.g.
188 Quinchilca and Bueno rivers, Figure 2b).

189 The local stratigraphy at the upper river course is formed by deposits originating in glacio-
190 lacustrine and glacio-fluvial environments, inherited from the last glacial and interglacial
191 periods, and the current postglacial. Rodríguez et al. (1999) indicate that in this zone the moraine
192 deposits intercalate with glacio-fluvial sediments and glacio-deformed laminated silts, which was
193 also observed by Davis and Karzulovic (1961) in the scarp that generated the largest slide of
194 1960 (~60 m, Figure S1a). Results of laboratory tests performed on sediments obtained from two
195 drillings, showed that some of the strata are susceptible to liquefaction (Noguera and Garcés,
196 1991). These authors propose that the deposits that were liquefied during the 1960 earthquake

197 correspond to perturbed silty strata with some sands and gravels, observable at ~28 m depth.
 198 This type of sediment combination (silt, sand and gravels) can also be seen in the scarp, between
 199 ~19 and 29 m deep (Figure S1b).



200 **Figure 2.** (a) Study area and San Pedro basin. (b and c) MMDs in the upper and middle course of
 201 San Pedro River. (d) Landform shaped by retrograde erosion generated by improper management
 202 of land use after the 1960 earthquake.

203 3 Materials and Methods

204 3.1 Historic archives

205 We conducted a research of historical sources to improve our knowledge about the MM deposits
 206 that dammed the San Pedro River in 1575. In addition to reviewing bibliography in recent
 207 scientific and historical works, we searched for documents in *the Archivo General de Indias*
 208 located in Seville, Spain; the *Archivo de la Nación* located in Lima, Peru; and the *Archivo*
 209 *Nacional* that is located in Santiago, Chile.

210 The *Archivo General de Indias* has a thousand of documents from Hispanic America, written in
 211 the times of the Conquest and Cologne. Most of these documents were addressed to the Kings
 212 and the authorities that ruled America from Spain. The *Archivo de la Nación* contains lodged
 213 manuscripts generated in the Governorships and Captaincies belonging to the Viceroyalty of
 214 Peru, including Chile, and which were directed towards authorities who lived in America as the
 215 Viceroy. Finally, the *Archivo Nacional* is the most important historical archive in Chile, and
 216 contains records issued to local authorities. In the latter we found three unpublished manuscripts
 217 that refer to the MM that dammed the San Pedro River in 1575, and that we describe in Table 1
 218 and in the supplementary material (Texts S1, S2 and S3).

219 3.2 Spatio-temporal characterization of MM deposits

220 The MM deposits in the San Pedro River were characterized by combining field observations,
 221 satellite images and early geomorphological descriptions of Davis and Karzulovic (1961).

222 Two fields surveys, conducted in January 2014 and 2015, were focused on the geomorphology
 223 and sedimentology characterization of the main MM deposits present in the upper course of the
 224 San Pedro River, and also in the outflow of Riñihue Lake. For the analysis of satellite images, we
 225 used the Google Earth software and images obtained by the Chilean Air Force in 1961, i.e. a few
 226 months after the 1960 earthquake occurred. For the geological description, the study by Davis
 227 and Karzulovic (1961) was used, complemented with the geological maps generated by
 228 Rodríguez et al. (1999).

229 We studied the evolution of the larger slide deposit generated by the 1960 earthquake using two
 230 topographic profiles obtained by Davis and Karzulovic (1961). Its location was georeferenced by
 231 means of a GIS (open source software QGIS) and was compared with two profiles obtained from
 232 a cloud of LIDAR points in 2010 (Figure 3a). The LIDAR information was processed with GIS,
 233 allowing the removal of the dense vegetation from the surface. As a result of this processing, a
 234 Digital Terrain Model (DTM) of 1 m of resolution was generated. The profiles were also
 235 obtained from other MM deposits present on the riverside zone of the San Pedro River, using the
 236 methodology described above.

237 3.3 Erosion rate of LT3 scarp

238 We studied the erosion rate along the largest slide deposit generated by the 1960 earthquake,
 239 hereafter referred to as LT3. The Erosion Rate (E), defined as the annual amount of eroded
 240 material from the scarp that forms part of LT3, was estimated from:

$$E = \frac{M}{t}$$

(1)

241 where M is the amount of mass removed from the scarp and t is the elapsed time. The period
242 considered is 50 years, between 1960 and 2010. The input for this calculation was obtained from
243 the two topographic profiles (A-A' and B-B', Figure 4b) reported in the paper of Davis and
244 Karzulovic (1961), and from LIDAR information processed in the GIS. Only the surface of the
245 escarpment was considered. As a result, two values of E were obtained, one for each topographic
246 profile and associated scarp.

247 Our calculations also considered depth-dependent changes of the density of the deposits that
248 formed the scarp. We use the densities present in Noguera and Garcés (1991), that were obtained
249 by drillings executed on the terrace where LT3 originated, close to main scarp. The density of
250 sediments changes significantly at 16 m depth. Therefore, a density $\rho=1.78$ tons/m³ and a $\rho=2.38$
251 tons/m³ was considered for the upper part and for the rest of the scarp, respectively. Finally, the
252 mass removed from the scarp was obtained by computing the weighted average between the
253 eroded volume and its respective density.

254 **4 History of MM that dammed the San Pedro River**

255 4.1 The MM triggered by the 1575 and 1960 earthquakes

256 The San Pedro River has been dammed at least twice since the beginning of written history of
257 Chile (i.e., 1541). In both occasions the trigger was strong shaking caused by earthquakes; first
258 in 1575 and then in 1960. Although multiple MM were reported for the 1960 earthquake at
259 different locations in south-central Chile (Weischet, 1963; Wright and Mella, 1963), those in the
260 San Pedro River reached public notoriety due to the threat that represented for the population of
261 ~60,000 inhabitants located downstream. Three slides dammed the river. The volumes of
262 sediments removed by these slides were 30×10^6 , 6×10^6 and 2×10^6 m³ (Davis and Karzulovic,
263 1961). The deposits that dammed the river were called locally as *Taco 3* (LT3), *Taco 2*
264 (hereinafter LT2), and *Taco 1* (hereinafter LT1) respectively (Figure 2c). Through the
265 intervention of the State of Chile (National Electric Company) and the heroic effort of hundreds
266 of locals, the dams were opened in a controlled manner. All these events, and due to the
267 proximity to Riñihue Lake, led to locals call this historic event as *Riñihuazo*.

268 In 1575, however, the population was severely affected, mainly those that lived on the riverside
269 zone. The historical chronicles compiled by Montessus de Ballore (1912) and Cisternas et al.
270 (2005) describe that the formation of the natural dam caused water accumulation for nearly five
271 months, collapsing catastrophically and the resulting outburst flood taking the lives of 800 to
272 1200 aborigines, according to data estimated by colonial authorities and witnesses. However,
273 none of the authors of the chronicles compiled by Montessus de Ballore described the MM that
274 blocked the river. Based on morphological features, Davis and Karzulovic (1961) proposed that
275 one of the deposits present in the upper course of the San Pedro River, which triples in size to
276 LT3, corresponds to the MM occurred in 1575 (Figure 2c). However, the historical evidence
277 presented below does not match with what was proposed by these authors.

278 4.2 Historical evidence of the characteristics of the MM of 1575

279 Our bibliographic and archive search resulted in nine historical documents that refer to the
280 deposit of 1575 event (Table 1). Among these, one written by an anonymous author provides the

281 only direct observations of the MM deposit when the San Pedro River was still dammed. The
 282 report describes both its size and location. Interestingly, both the size and location inferred from
 283 this first-hand account do not coincide with those suggested by Davis and Karzulovic (1961)
 284 based on morphological appearances. The MM deposit suggested by these authors is located 2
 285 km away from the outflow of Riñihue Lake (Figure 2c). However, the eyewitness reported a
 286 location right in the outflow of Riñihue Lake, and an associated volume of $\sim 1.2 \times 10^6 \text{ m}^3$ and an
 287 area of $\sim 1,5 \text{ ha}$ (according to the official measurement unit used in those years (e.g., De Ramon
 288 and Larraín, 1979)), which is about half the volume of LT1 and ~ 200 times smaller than the
 289 landslide proposed by Davis and Karzulovic (1961). Seven other secondary sources support the
 290 location reported by the eyewitness (Table 1).

291 Table 1

292 *Historical data obtained from settlers of the MM of 1575*

Type of historical source	Author	Place of origin	Date	Eyewitness?	N° of MM described	Location	Size of MM	Lake level rise	Source
Letter	Pedro Feyjó	Valdivia	12/28/1575	No	1	Outflow of Riñihue Lake	-	-	in Cisternas et al., 2005
Letter	Cabildo de la Imperial	La Imperial	01/08/1576	No	2	Outflow of Riñihue Lake	-	-	in Cisternas et al., 2005
Letter	Martín Ruiz de Gamboa	Concepción	02/12/1576	No	-	Outflow of Riñihue Lake	-	-	in Cisternas et al., 2005
Letter	Francisco de Gálvez	Santiago	02/21/1576	No	2	-	-	-	Unpublished. See in supplementary Text S1
Relation	Anonymous	-	Between dec. 1575 and apr. 1576	No	-	Outflow of Riñihue Lake	-	$\sim 70 \text{ m}$	in Silgado, 1985
Letter	Antonio Carreño	Santiago	08/10/1576	No	-	Outflow of Riñihue Lake	-	$\sim 80 \text{ m}$	Unpublished. See in supplementary Text S2
Relation	Antonio Carreño	Santiago	10/10/1576	No	-	Outflow of Riñihue Lake	-	$\sim 80 \text{ m}$	Unpublished. See in supplementary Text S3
Chronicle	Pedro Mariño de Lobera	Santiago	-	No	1	Outflow of Riñihue Lake	-	-	in Montessus de Ballore, 1912; in Cisternas et al., 2005
Relation	Anonymous	Arauco Province	Between 1576-1598	Yes	1	Outflow of Riñihue Lake	$\sim 1 \times 10^6 \text{ m}^3$ *	$\sim 50 \text{ m}$	in Silgado, 1985

293 *1x1 quarter pace and 30 “*estados*” high.

294 **5 Characteristics and evolution of LT3**

295 5.1 The sliding process

296 The deposit of LT3 was generated by a multirotational slide (Hauser, 2002). At the time of its
297 formation the slide generated an average scarp of 40 m. The slide deposit was made up of a
298 debris apron, a series of failed and rotated blocks, a large unitary block, folds, and a terminal
299 zone or toe, corresponding to the propagation front that went towards the San Pedro River
300 (Figure 3a). The toe and the unitary block were the sections of slide that dammed the riverbed.
301 The toe was eroded by the river after the works carried out for the controlled opening of the
302 *Tacos*, modifying the original course.

303 In the first months after the slide, important erosive processes and deposits such as pediments,
304 cones, fans, deltas, drainage systems and block rounding were observed (Davis and Karzulovic,
305 1961). This was caused by the abundant precipitation, the initial absence of vegetation and the
306 presence of a large number of water springs that arose from the different porous sediments of the
307 escarpment wall, discharging water towards the slide deposit.

308 5.2 The Evolution of LT3

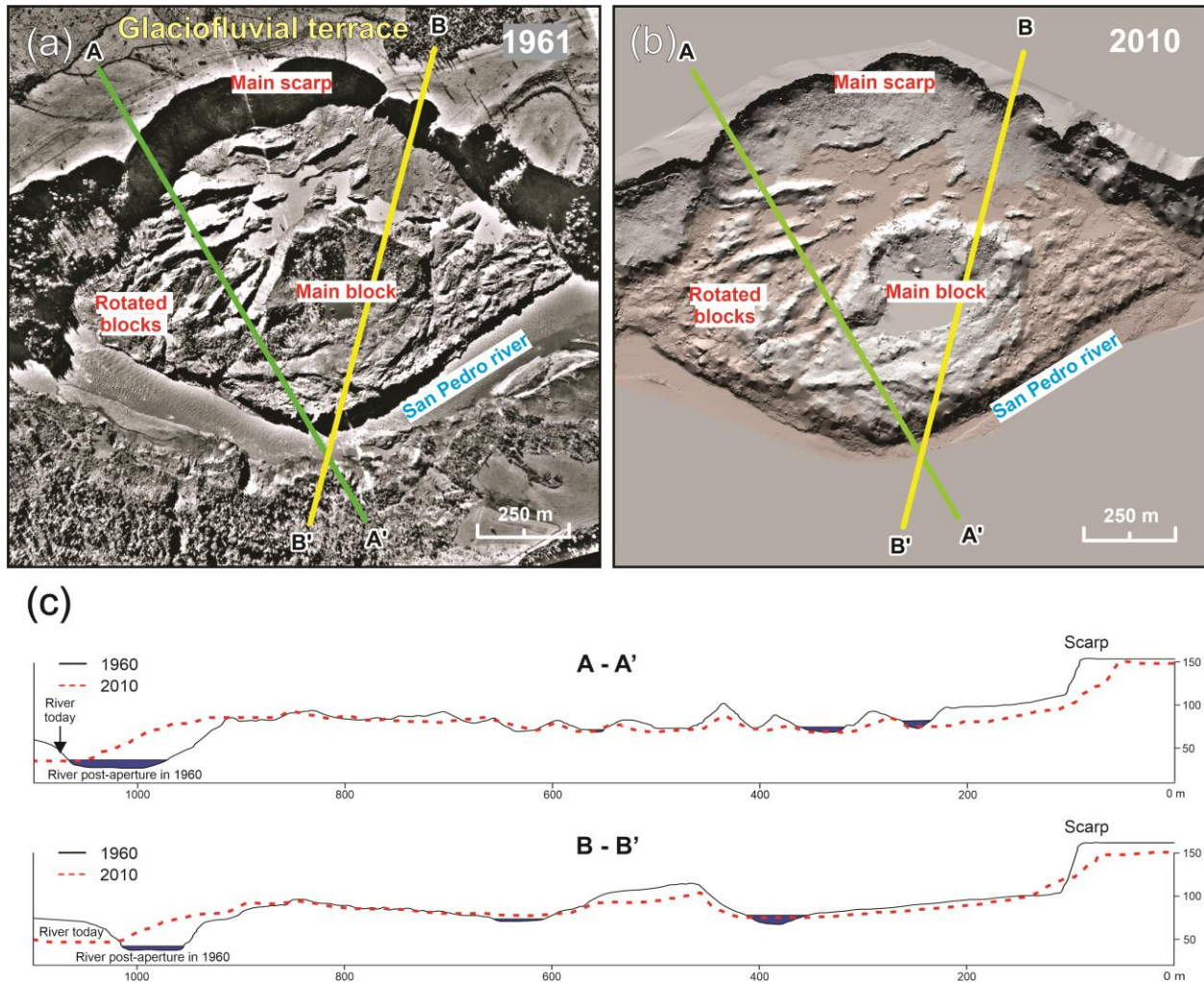
309 The profiles presented in Figure 3c show that, in 50 years, the landform show important changes
310 is the main scarp, since it shows a notable setback and a decrease in its slope gradient (see
311 section 5.3). The other main structures of the landslide deposit, such as the rotated blocks and the
312 unit block, have been preserved without major changes. Only a softening and lowering of its
313 slopes is observed. Some lagoons formed in 1960 still persist, while the others have been filled
314 with sediments and/or drained. Moreover, vegetation coverage has increased in height and
315 density. The bed of the San Pedro River is displaced towards the south for about 70 m (Figure
316 3c), possibly caused by a lateral displacement of the slide deposit. This phenomenon, in
317 conjunction with the occurrence of dams, indicates that the upper course of the San Pedro River
318 undergoes significant modifications in its shape and axis due to earthquake-triggered MM and
319 the post-depositional mobility of the MM deposits.

320 5.3 Scarp retreat

321 The scarp of the B-B' profile has a higher erosive rate than the scarp of A-A' (Figure 3c). The A-
322 A' scarp presents an average erosion rate of 39 tons/year per linear meter of scarp, while the B-B'
323 scarp averages a rate of 58 tons/year. This erosive rate is also reflected in the slope changes
324 experienced by the escarpment: from 71° to 43° for A-A', and from 75° to 37° for B-B'. It should
325 be considered that the escarpment of the B-B' profile had a greater height (10 m) and slightly
326 steeper initial gradient.

327 According to descriptions of Davis and Karzulovic (1961), it is inferred that in 1960 the erosion
328 index was much higher than the averages described above, because at present the same erosive
329 phenomena described by these authors are not observed (see section 4.1). The difference and
330 variability between erosive indices hampers the morphologic dating of the MM deposits in the
331 study area, due to more homogeneous value is needed in a scarp formed at the same time or

332 event. Additionally, some escarpments can be reactivated and/or accelerate their erosive
 333 processes with the occurrence of earthquakes subsequent to their formation (see section 6.1).



334 **Figure 3.** (a) LT3 main geomorphological features in aerial photography (Chilean Air Force,
 335 1961) and (b) 2010 LT3 DTM LIDAR-based information. (c) Topographic profiles (profiles
 336 lines in A and B) obtained from Davis and Karzulovic (1961) (A-A'/B-B') compared to profiles
 337 obtained from LIDAR-based information.

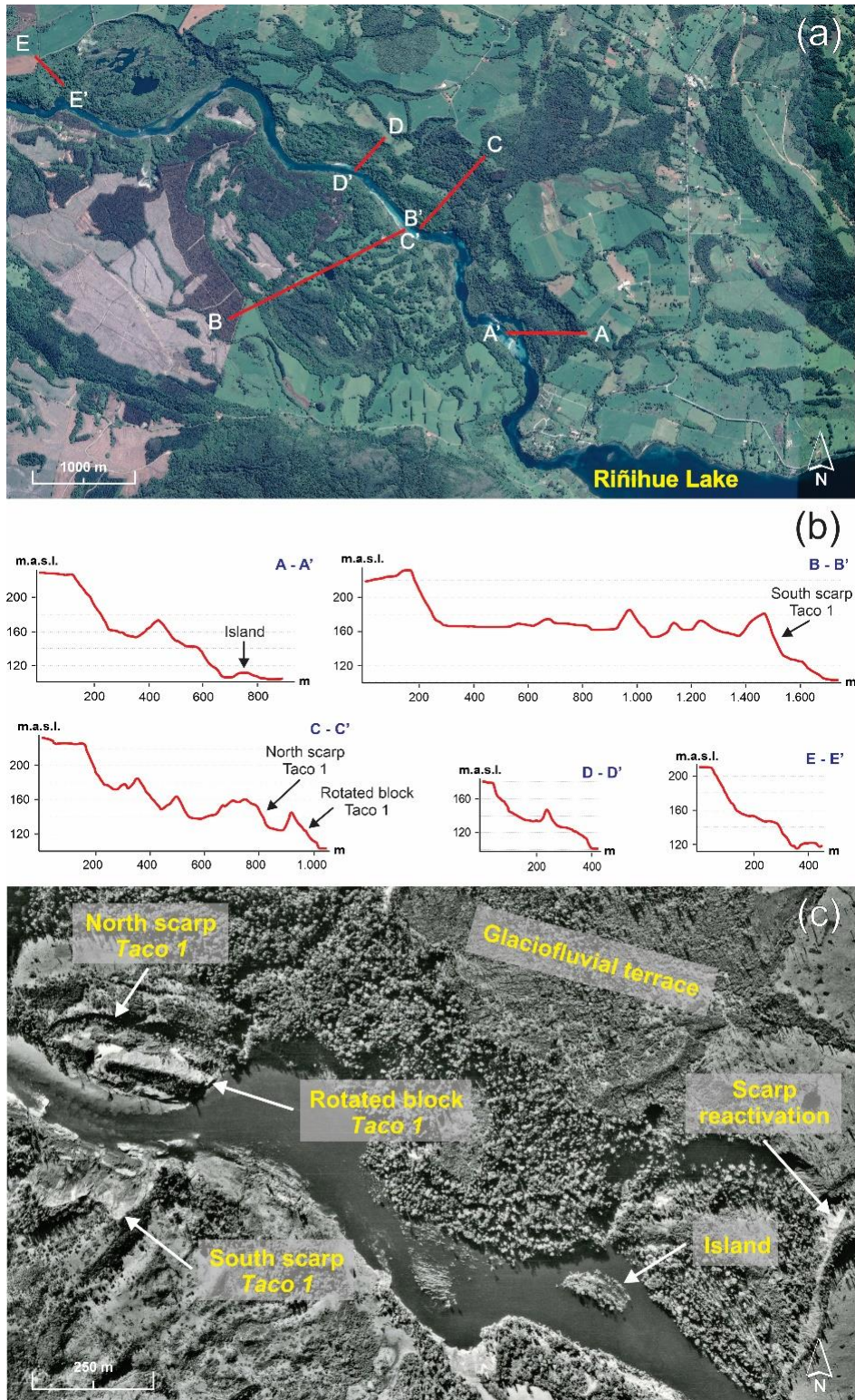
338 6 Ancient MM deposits as evidence of recurrent earthquakes

339 6.1 Characteristics of ancient MM deposits in the San Pedro river upper course

340 By screening historical documents, we could not find evidence of other processes of dam
 341 formation (and subsequent outburst floods) in the San Pedro River other than by earthquakes.
 342 This leads us to believe that the ancient deposits (generated before 1960) in the riverside zone of
 343 the San Pedro River were also formed by earthquakes. Morphological similarities with those
 344 generated in 1960 further support this suggestion.

345 Traces of the ancient deposits, potentially associated to earthquake-induced MM, are shown in
346 Figure 4. Among their main characteristics, they feature escarpments of 20 m or more with
347 slopes above 30° and exhibit a slide body that projects into the river with one or more ridges.
348 Two of the ancient MM deposits (visualized in B-B' and C-C' profiles, Figure 4b) were modified
349 by the 1960 earthquake, because the slides that generated the LT1 were formed on a section of
350 these (Figure 4c). In contrast, the deposit of the LT2 represented in the D-D' profile (Figure 4b)
351 was originated entirely by the 1960 earthquake. The deposits represented by the A-A' and E-E'
352 profiles in the Figure 4b have morphological characteristics similar to the other deposits
353 previously described, and presented reactivations of their scarps during the 1960 earthquake,
354 which can be observed for the E-E' profile in Figure 4b. All the elements described above
355 suggest that, although some deposits may have been formed in a single event, others were caused
356 by remobilizing preexisting MM deposits.

357 This data suggests that a MM deposit can be formed by one or more events generated at different
358 times. If the historical antecedents (size and location) are considered, the proposal of Davis and
359 Karzulovic (1961) for the 1575 MM becomes even more debatable, because the proposed deposit
360 can be made up of more than two events. The deposit represented by A-A' profile in Figure 4b is
361 located closer to the Riñihue Lake outflow and its section bordering the river could be
362 considered as a more possible candidate for the 1575 river-damming MM deposit. This
363 hypothesis considers the morphology, the size and the location revealed by the historical
364 evidence, in addition to the presence of an island as a typical characteristic of MM deposits in
365 this locality (section 6.2; Figure 5).



366 **Figure 4.** (a and b) MM deposit profiles in San Pedro River upper course. (c) Scarps of slide
 367 deposit that generated LT1 and evidence of reactivation of scarps of ancient MM by the 1960
 368 earthquake (Aerial photography from Chilean Air Force, 1961).

369 6.2 Islands as evidence of ancient MM?

370 The islands along the upper and middle course of the San Pedro River may have been formed
 371 from ancient MM as well. Similar islands formed by MM have also been observed by Hewitt
 372 (1998) in the upper course of the Indus River in Pakistan. One of the islands in the upper course
 373 of the San Pedro River was investigated in the field and has characteristics that suggest a
 374 colluvial and non-fluvial origin. Its location (facing an ancient MM deposit), size, geological
 375 composition, and the low sediment load of the river support this proposal (island in Figure 5b
 376 and 5c).

377 The island currently has an area of ~1.4 ha, a height of ~4 m above the average water level of the
 378 river and shows a dense vegetation on its surface. The island existed before the 1960 event
 379 (Figure 4c), so it resisted at least partially, the increase in the water level and controlled
 380 discharge in the river during the *Riñihuazo*. Its presence is remarkable considering that the upper
 381 course of the San Pedro River is devoid of sediment load as Riñihue Lake and the other lakes
 382 upstream act as sediment traps. This situation, combined with other factors such as slope and
 383 average flow (1% / ~400 m³/s) determine the presence of bedforms, such as middle and lateral
 384 banks. The island deposits consist of glaciofluvial terrace material and morainic deposits, which
 385 is similar to MM deposits located alongside the San Pedro River. This idea is supported by the
 386 granulometric variability (very poor sorting) and the existence of rounded to sub-rounded blocks
 387 in a matrix of fine sediments (silts and clays) and gravels (Figure 5b and 5c).

388 All in all, these observations may suggest that this island was part of an ancient MM that could
 389 have dammed the San Pedro River. Also, it leads us to suggest that the other islands located
 390 further downstream, which face ancient MM deposits, are vestiges of these and not fluvial
 391 deposits.



392 **Figure 5.** Deposits in an island in the upper course of San Pedro River suggesting that it was
 393 formed by an ancient MM that dammed the river.

394 7 Factors that affect the generation of MM in the San Pedro River

395 As reviewed in the previous sections, the 1575 and 1960 earthquakes must have generated
396 sufficient local intensities to trigger MM capable of damming the upper course of San Pedro
397 River. Stronger shaking from these events, compared with the rest of the historical sequence, is
398 consistent with the turbidite record in Riñihue Lake and other nearby lakes (Moernaut et al.,
399 2014). Based on the similar thickness and distribution of the 1575 and 1960 turbidite deposits,
400 Moernaut et al. (2014) inferred seismic intensities of about MMI VII½ for the 1575 earthquake
401 in Riñihue Lake. On the other hand, in the 1737 and 1837 earthquakes there were no MM that
402 dammed the San Pedro River, and coincidentally, the inferred seismic intensities based on the
403 Riñihue Lake sedimentary record were smaller (about VI½) for these earthquakes (Moernaut et
404 al., 2014).

405 Considering these facts, from the point of view of the analysis of Natural Hazards it is necessary
406 to ask: What are the factors that influence the triggering of MM in the upper section of the San
407 Pedro River, and what are the scenarios capable of triggering MM in this zone? If we assume
408 that geological and seismic conditions are relatively constant in a period of a few millennia, then
409 it is reasonable to consider climate seasonality, transient climatological events (e.g. ENSO
410 events), geomorphological evolution and land use as factors that affect the generation, quantity
411 and dimensions of MM. In the case of the San Pedro River, the incidence of the seasons and land
412 use can be evaluated, because although Moernaut et al. (2014) assign similar seismic intensities
413 between the earthquakes of 1575 and 1960, the historical evidence reveals variations regarding
414 the quantity and size of the MM that they generated. If we consider the testimony of the only
415 known eyewitness (see 4.2 section), the 1575 earthquake generated a single MM deposit that
416 reached an approximate dimension of about $1.2 \times 10^6 \text{ m}^3$, equivalent to half the size of the slide
417 generated by LT1, and 1/30 of LT3.

418 The area in which the upper course of the San Pedro River is located is one of the rainiest in
419 south-central Chile. According to the Chilean General Direction for Water, it rains annually
420 ~2200 mm, focused mainly during autumn and winter (Riñihue Lake station, General Direction
421 for Water, 2019). The 1960 earthquake occurred in autumn on May 22, and the annual rainfall
422 accumulated up to that date was 580 mm (Chilean Meteorological Direction, 2019). This amount
423 of accumulated rainfall favored a saturation of the fine sensitive strata, being decisive for the
424 generation of slides on nearly-horizontal strata (Noguera and Garcés, 1991). In contrast, the
425 event of 1575 occurred in December 16, that is, entering the summer, so that strata may have
426 been saturated to a much smaller degree than in case of the 1960 event. Possibly, these seasonal
427 variations partly explain the differences in quantity and size of deposits generated by the events
428 of 1575 and 1960.

429 As was recently demonstrated by the September 2018 Mw 7.5 earthquake in Sulawesi,
430 Indonesia, inefficient land use management combined with strong shaking events can cause
431 catastrophic consequences for the population due to MM (Watkinson and Hall, 2019; Bradley et
432 al., 2019). In general, less vegetation cover on non-rocky slopes condition the saturation of the
433 strata and the water table, making them more susceptible to failure (Wu and Sidle, 1995). In
434 1575, there is no evidence of settlements or significant extractive activities in the upper course of
435 the San Pedro River, neither Spanish nor indigenous, so the forest vegetation was practically
436 pristine (Solarí et al., 2011). Whereas for 1960, the aerial photographs show grasslands with

437 subdivisions and soil with scarce arboreal vegetation (agricultural use), as can be seen in the
 438 glaciofluvial terrace where LT3 was formed (Figure 3a). Therefore, it is reasonable to think that
 439 the slopes and surfaces in 1575 could have been less susceptible to failure than in 1960, as a
 440 result of the greater vegetational coverage and the better condition of the soils, which in turn
 441 allowed for less infiltration and saturation of pores in the strata. These differences suggest that
 442 the MMs that originated the *Riñihualzo* in 1960 may not have occurred in such quantity and
 443 magnitude if the earthquake would have occurred in a drier season and/or with less human
 444 intervention, as in 1575. In any case, MM and river damming occurred regardless of the season
 445 or land use, so these aspects may be less important than the seismic or geological factors.

446 **8 Conclusions**

447 Here we suggest that in the present conditions not only a giant earthquake (Mw 9-type) like in
 448 1575 or 1960 is needed to dam the San Pedro River, but that also a medium-size earthquake (Mw
 449 about 8) could do this. We base this on the following reasoning: i) the geological conditions of
 450 the upper course of the San Pedro River which facilitate the development of slope failures and
 451 reactivations of MM deposits; ii) the current seismic condition of the Valdivia segment that has
 452 already the potential to generate earthquakes of magnitude ~8 (Moernaut et al., 2018; Moreno et
 453 al., 2018); iii) the precipitation regime (~2200 mm/yr) with excessive rainfall in winter; iv) the
 454 land use which has caused the development of a significant landform (4 ha) shaped by retrograde
 455 erosion, generated by improper management (Figure 2c and 2d); v) and the historical evidence
 456 that shows us that relatively small MM can dam the San Pedro River, such as the LT1 of 1960
 457 and the MM deposit described in 1575.

458 The evidence presented here has important implications for the engineering design and
 459 emergency plan (in case of a new landslide dam and potential outburst flood) of the hydroelectric
 460 power plant located 6 km downstream of LT3, and that is currently being evaluated by the
 461 Chilean Environmental Assessment System.

462 **9. Acknowledgments**

463 C.A.C. acknowledges the support of the Doctoral program of Institute of Geography of the
 464 Pontificia Universidad Católica de Chile. M.C. acknowledges the support of the Iniciativa
 465 Científica Milenio (ICM) through Grant Number NC160025, FONDECYT Project Number
 466 1190258, and the doctoral program of Geological Sciences of the Universidad de Concepción.
 467 Special thanks to F. Torrejón for his collaboration in the search for unpublished historical
 468 information and his references to information already published.

469 **10. Bibliography**

- 470 Agurto, H., Rietbrock, A., Barrientos, S., Bataille, K., & Legrand, D. (2012). Seismo-tectonic
 471 structure of the Aysén Region, Southern Chile, inferred from the 2007 Mw = 6.2 Aysén
 472 earthquake sequence. *Geophysical Journal International*, 190(1), 116-130. doi:
 473 10.1111/j.1365-246X.2012.05507.x
- 474 Alexander, D. (2012). Vulnerability to Landslides. In T. Glade, M. Anderson & M. J. Crozier
 475 (Eds.), *Landslide Hazard and Risk* (pp. 175-198): John Wiley & Sons, Ltd.

- 476 Alvarado, P., Barrientos, S., Saez, M., Astroza, M., & Beck, S. (2009), Source study and tectonic
477 implications of the historic 1958 Las Melosas crustal earthquake, Chile, compared to
478 earthquake damage. *Phys. Earth Planet. Inter.*, 175, 26-36.
479 doi:10.1016/j.pepi.2008.03.015
- 480 Angermann, D., Klotz, J., & Reigber, C. (1999). Space-geodetic estimation of the Nazca-South
481 America Euler vector. *Earth and Planetary Science Letters*, 171(3), 329-334.
- 482 Antinao, J. L., & Gosse, J. (2009). Large rockslides in the Southern Central Andes of Chile (32–
483 34.5°S): Tectonic control and significance for Quaternary landscape evolution.
484 *Geomorphology*, 104(3), 117-133. doi: 10.1016/j.geomorph.2008.08.008
- 485 Astroza, M., Moya, R., & Sanhueza, S. (2002). Estudio comparativo de los efectos de los
486 terremotos de Chillan de 1939 y de talca de 1928. Paper presented at the VIII Jornadas
487 Chilenas de Sismología e Ingeniería Antisísmica, Valparaíso, Chile.
- 488 Astroza, M., & Lazo, R. (2010). Estudio de los daños de los terremotos del 21 y 22 de Mayo de
489 1960. Paper presented at the X Jornadas de Sismología e Ingeniería Antisísmica,
490 Santiago, Chile.
- 491 Astroza, M., Ruiz, S., & Astroza, R. (2012). Damage Assessment and Seismic Intensity Analysis
492 of the 2010 (M-w 8.8) Maule Earthquake. *Earthquake Spectra*, 28. doi:
493 10.1193/1.4000027
- 494 Barnhart, W. D., Hayes, G. P., & Wald, D. J. (2019). Global Earthquake Response with Imaging
495 Geodesy: Recent Examples from the USGS NEIC. *Remote Sensing*, 11(11), 1357.
- 496 Beck, S., Barrientos, S., Kausel, E., & Reyes, M. (1998). Source characteristics of historic
497 earthquakes along the central Chile subduction Askew et Alzone. *Journal of South
498 American Earth Sciences*, 11(2), 115-129.
- 499 Bradley, K., Mallick, R., Andikagumi, H., Hubbard, J., Meilianda, E., Switzer, A., . . . Benazir,
500 B. (2019). Earthquake-triggered 2018 Palu Valley landslides enabled by wet rice
501 cultivation. *Nature Geoscience*, 1-5.
- 502 Budimir, M. E. A., Atkinson, P. M., & Lewis, H. G. (2014). Earthquake-and-landslide events are
503 associated with more fatalities than earthquakes alone. *Natural Hazards*, 72(2), 895-914.
504 doi: 10.1007/s11069-014-1044-4
- 505 Carvajal, M., Araya-Cornejo, C., Sepúlveda, I., Melnick, D., & Haase, J. S. (2018). Nearly
506 instantaneous tsunamis following the Mw 7.5 2018 palu earthquake. *Geophysical
507 Research Letters*, 46(10): 5117-5126. doi: 10.1029/2019gl082578
- 508 Carver, G., Plafker, G., Metz, M., Cluff, L., Slemmons, B., Johnson, E., . . . Sorensen, S. (2004).
509 Surface Rupture on the Denali Fault Interpreted from Tree Damage during the 1912 Delta
510 River Mw 7.2–7.4 Earthquake: Implications for the 2002 Denali Fault Earthquake Slip
511 Distribution. *Bulletin of the Seismological Society of America*, 94(6B), S58-S71. doi:
512 10.1785/0120040625

- 513 Cisternas, M., Atwater, B. F., Torrejón, F., Sawai, Y., Machuca, G., Lagos, M., . . . Kamataki, T.
514 (2005). Predecessors of the giant 1960 Chile earthquake. *Nature*, 437(7057), 404.
- 515 Cisternas, M., Carvajal, M., Wesson, R., Ely, L. L., & Gorigoitia, N. (2017a). Exploring the
516 Historical Earthquakes Preceding the Giant 1960 Chile Earthquake in a Time-Dependent
517 Seismogenic Zone. *Bulletin of the Seismological Society of America*, 107(6), 2664-2675.
518 doi: 10.1785/0120170103
- 519 Cisternas, M., Garrett, E., Wesson, R., Dura, T., & Ely, L. (2017b). Unusual geologic evidence
520 of coeval seismic shaking and tsunamis shows variability in earthquake size and
521 recurrence in the area of the giant 1960 Chile earthquake. *Marine Geology*, 385, 101-113.
- 522 Colombelli, S., Allen, R. M., & Zollo, A. (2013). Application of real-time GPS to earthquake
523 early warning in subduction and strike-slip environments. *Journal of Geophysical*
524 *Research: Solid Earth*, 118(7), 3448-3461. doi: 10.1002/jgrb.50242
- 525 Davis, S., & Karsulovic, J. (1961). *Deslizamientos en el valle del río San Pedro provincia de*
526 *Valdivia, Chile*. Paper presented at the Anales de la Facultad de Ciencias Físicas y
527 Matemáticas.
- 528 Dura, T., Horton, B.P., Cisternas, M., Ely, L., Hong, I., Nelson, A.R., Wesson, R.L., Pilarczyk,
529 J.E., Parnell, A.C., Nikitina, D. (2017). Subduction zone slip variability during the last
530 millennium, south-central Chile. *Quat. Sci. Rev.* 175, 112e137.
- 531 De Ramón, A. & Larraín, J. (1979). Una metrología colonial para Santiago de Chile: de la
532 medida castellana al sistema métrico decimal. *Historia (Santiago: Instituto de Historia,*
533 *Pontificia Universidad Católica de Chile)*, 14, 5-71.
- 534 General Direction for Water. (2019). Official Hydrometeorological and Water Quality
535 Information Online. <http://snia.dga.cl/BNAConsultas/reportes>
- 536 Gorum T., Fan X., van Westen, C.J., Huang, R.Q., Xu Q., Tang, C., & Wang, G. (2011).
537 Distribution pattern of earthquake-induced landslides triggered by the 12 May 2008
538 Wenchuan earthquake. *Geomorphology*, 133(3-4):152–167. doi:
539 10.1016/j.geomorph.2010.12.030
- 540 Habit, E., & Parra, O. (2012). Fundamento y aproximación Metodológica del Estudio de peces
541 del Río San Pedro. *Gayana (Concepción)*, 76, 01-09.
- 542 Harp, E. L., Keefer, D. K., Sato, H. P., & Yagi, H. (2011). Landslide inventories: the essential
543 part of seismic landslide hazard analyses. *Engineering Geology*, 122(1-2), 9-21.
- 544 Hauser, A. (2000). *Remociones en masa en Chile (versión actualizada)*: Servicio Nacional de
545 Geología y Minería.
- 546 Hewitt, K. (1998). Catastrophic landslides and their effects on the Upper Indus streams,
547 Karakoram Himalaya, northern Pakistan. *Geomorphology*, 26(1-3), 47-80.

- 548 Kanamori, H., & Cipar, J. (1974). Focal process of the great Chilean earthquake May 22, 1960.
549 *Physics of the Earth and Planetary Interiors*, 9(2), 128-136.
- 550 Keefer, D. (1984). Landslides caused by earthquakes. *GSA Bulletin*, 95(4), 406-421. doi:
551 10.1130/0016-7606(1984)95<406:LCBE>2.0.CO;2
- 552 Keefer, D. (2013). 5.11 Landslides Generated by Earthquakes: Immediate and Long-Term
553 Effects. In J. F. Shroder (Ed.), *Treatise on Geomorphology* (pp. 250-266). San Diego:
554 Academic Press.
- 555 Keefer, D., & Larsen, M. (2007). Assessing Landslide Hazards. *Science*, 316, 1136-1138. doi:
556 10.1126/science.1143308
- 557 Lay, T., Kanamori, H., Ammon, C. J., Koper, K. D., Hutko, A. R., Ye, L., . . . Rushing, T. M.
558 (2012). Depth-varying rupture properties of subduction zone megathrust faults. *Journal*
559 *of Geophysical Research: Solid Earth*, 117(B4). doi: 10.1029/2011jb009133
- 560 Lomnitz, C. (1970). Major earthquakes and tsunamis in Chile during the period 1535 to 1955.
561 *Geologische Rundschau*, 59(3), 938-960. doi: 10.1007/bf02042278
- 562 Mardones Flores, M., & Rojas Hernández, J. (2012). Procesos de remoción en masa inducidos
563 por el terremoto del 27F de 2010 en la franja costera de la Región del Biobío, Chile.
564 *Revista de Geografía Norte Grande*(53), 57-74.
- 565 Meteorological Direction of Chile. (2019). Climatological Yearbook.
566 <https://climatologia.meteochile.gob.cl/application/index/anuarios>
- 567 Moernaut, J., Daele, M. V., Heirman, K., Fontijn, K., Strasser, M., Pino, M., . . . De Batist, M.
568 (2014). Lacustrine turbidites as a tool for quantitative earthquake reconstruction: New
569 evidence for a variable rupture mode in south central Chile. *Journal of Geophysical*
570 *Research: Solid Earth*, 119(3), 1607-1633. doi: 10.1002/2013jb010738
- 571 Moernaut, J., Van Daele, M., Fontijn, K., Heirman, K., Kempf, P., Pino, M., Valdebenito, G.,
572 Urrutia, R., Strasser, M., De Batist, M. 2018. Larger earthquakes recur more periodically:
573 New insights in the megathrust earthquake cycle from lacustrine turbidite records in
574 south-central Chile. *Earth and Planetary Science Letters* 481, 9-19.
- 575 Montessus de Ballore, F. (1912). Historia sísmica de los Andes Meridionales al sur del paralelo
576 XVI. Segunda parte. Imprenta Cervantes. *Santiago*.
- 577 Moreno, M., Li, S., Melnick, D., Bedford, J., Baez, J., Motagh, M., . . . Gutknecht, B. (2018).
578 Chilean megathrust earthquake recurrence linked to frictional contrast at depth. *Nature*
579 *Geoscience*, 11(4), 285.
- 580 National Seismological Center of Chile. (2019). Great earthquakes in Chile.
581 <https://www.csn.uchile.cl/sismologia/grandes-terremotos-en-chile/>

- 582 Noguera, C., & Garcés, E. (1991). *Deslizamiento en el río San Pedro, analizado 30 años*
583 *después*. Paper presented at the Memorias, 9o Congreso Panamericano de Mecánica de
584 Suelos e Ingeniería de Fundaciones, Viña del Mar, Chile.
- 585 Ojala, A. E., Mattila, J., Markovaara-Koivisto, M., Ruskeeniemi, T., Palmu, J.-P., & Sutinen, R.
586 (2017). Distribution and morphology of landslides in northern Finland: An analysis of
587 postglacial seismic activity. *Geomorphology*. doi: 10.1016/j.geomorph.2017.08.045
- 588 Rodríguez, C., Pérez, Y., Moreno, H., Clayton, J., Antinao, J., Duhart, P., & Martin, M. (1999).
589 Area de Panguipulli-Riñihue, Región de Los Lagos. *Servicio Nacional de Geología y*
590 *Minería, Mapas Geológicos, 10(1)*.
- 591 Ruiz, S., & Madariaga, R. (2018). Historical and recent large megathrust earthquakes in Chile.
592 *Tectonophysics, 733*, 37-56.
- 593 Scholz, C. H. (2002). *The Mechanics of Earthquakes and Faulting* (2 ed.). Cambridge:
594 Cambridge University Press.
- 595 Sepúlveda, S. A., Serey, A., Lara, M., Pavez, A., & Rebolledo, S. (2010). Landslides induced by
596 the April 2007 Aysén Fjord earthquake, Chilean Patagonia. *Landslides, 7(4)*, 483-492.
597 doi: 10.1007/s10346-010-0203-2
- 598 Serey, A., Piñero-Feliciangeli, L., Sepúlveda, S. A., Poblete, F., Petley, D. N., & Murphy, W.
599 (2019). Landslides induced by the 2010 Chile megathrust earthquake: a comprehensive
600 inventory and correlations with geological and seismic factors. *Landslides, 16(6)*, 1153-
601 1165. doi: 10.1007/s10346-019-01150-6
- 602 Silgado, E. (1985). Terremotos destructivos en America del Sur: 1530-1894. Centro Regional de
603 Sismología para America del Sur (CERESIS), 10, 328 p.
- 604 Symithe, S., & Calais, E. (2016). Present-day shortening in Southern Haiti from GPS
605 measurements and implications for seismic hazard. *Tectonophysics, 679*, 117-124.
- 606 U.S. Geological Survey (2016). M 7.6 - 41km SW of Puerto Quellon, Chile,
607 <https://earthquake.usgs.gov/earthquakes/feed/v1.0/detail/us10007mn3.kml>
- 608 Vanneste, K., Wils, K., & Van Daele, M. (2018). Probabilistic evaluation of fault sources based
609 on paleoseismic evidence from mass- transport deposits: the example of Aysén Fjord,
610 Chile. *Journal of Geophysical Research: Solid Earth, 123*, 9842–9865. [https://doi.org/](https://doi.org/10.1029/2018JB016289)
611 [10.1029/2018JB016289](https://doi.org/10.1029/2018JB016289)
- 612 Watkinson, I. M., & Hall, R. (2019). Impact of communal irrigation on the 2018 Palu
613 earthquake-triggered landslides. *Nature Geoscience, 1-6*.
- 614 Weischet, W. (1963). Further observations of geologic and geomorphic changes resulting from
615 the catastrophic earthquake of May 1960, in Chile. *Bulletin of the Seismological Society*
616 *of America, 53(6)*, 1237-1257.

617 Wright, C., & Mella, A. (1963). Modifications to the soil pattern of South-Central Chile resulting
618 from seismic and associated phenomena during the period May to August 1960.
619 *Bulletin of the Seismological Society of America*, 53(6), 1367-1402.

620 Wu, W., & Sidle, R. C. (1995). A Distributed Slope Stability Model for Steep Forested Basins.
621 *Water Resources Research*, 31(8), 2097-2110. doi: 10.1029/95wr01136

622